Numerical predictions of turbulent flow and heat transfer in circular pipes using a low Reynolds number two-equation model of turbulence

S. H. Chan[1], R. Amano[2], M. Abou-Ellail[2], S. Kaseb[3] & H. Kayed[3]
[1]*Fuel Cell Center, Yuan Ze University, Taiwan*
[2]*Mechanical Engineering Department,*
University of Wisconsin-Milwaukee, USA
[3]*Mechanical Engineering Department, Cairo University, Egypt*

Abstract

The present paper is concerned with the numerical simulations of the turbulent flow and heat transfer in circular pipes using a low Reynolds number model for turbulence kinetic energy and its dissipation rate. Unlike the high Reynolds number turbulence models, the present solution procedure requires no special treatments near the pipe walls; i.e., no wall functions are needed to simulate the turbulent flow and heat transfer at the pipe walls. It is well known that the type of the wall function has been criticized on the basis that the obtained solution is essentially dependent on some adjustable tuning model constants. The present low Reynolds number model takes the solution up to the walls without any abrupt changes in the axial velocity and temperature profiles. Finite-volume equations are derived for the conservation equations of the mass continuity, axial and radial velocity components, temperature, turbulence kinetic energy and its dissipation rate. The resulting finite-volume equations are solved iteratively using a tri-diagonal matrix algorithm. The obtained results are considered converged when the errors are less than 0.1 percent. The converged radial profiles of the gas temperature, the axial velocity and the axial profiles of the Nusselt number, mean bulk temperature and wall heat flux are presented for six fixed values of the Reynolds numbers. Moreover, the axial profiles of the Nusselt number are presented for six values of the Reynolds number. The

WIT Transactions on Engineering Sciences, Vol 68, © 2010 WIT Press
www.witpress.com, ISSN 1743-3533 (on-line)
doi:10.2495/HT100101

agreement between the present results and the corresponding standard analytical and numerical data is very good.

Keywords: numerical simulation, low Reynolds number, turbulent flow, heat transfer.

1 Introduction

The prediction of turbulent flows is a powerful tool both for academic studies and design of industrial applications [1–10]. The present work is concerned with predicting the turbulent flow and heat transfer in pipes. The pipe wall is kept at a constant temperature of 400 K. Six computer runs are performed, with each run having a constant Reynolds number. In order to remove the uncertainty of using wall functions, a low Reynolds number, two-equation, model of turbulence is adopted. This low Reynolds number model was developed by Launder and Sharma [11]. Other low Reynolds number models were assessed by Hrenya et al [12]. Here also the Launder and Sharma model is checked against, experimental data [13], semi-empirical power law [14] and the standard high Reynolds number $k-\varepsilon$ model with wall functions. These comparisons are performed at a value of Reynolds number equals to 500,000. Numerical solution procedures vary in accuracy from first-order difference equations with appraisable numerical errors to higher-order finite-difference schemes with lesser numerical diffusion. In the present work, the recent higher-order scheme of Abou-Ellail et al [3] is used. The computed low Reynolds number model results, for the fully-developed Nusselt number, are compared with the analytical equation of Holman [15].

2 Mathematical model

The governing equations for time-mean turbulent flows in circular pipes are presented in this section.

2.1 Continuity and momentum equations

The time-mean mass continuity equation may be written in tensor notations as:

$$\frac{\partial}{\partial x_i}(\rho \overline{u}_i) = 0 \tag{1}$$

The modeled time-mean momentum equation for turbulent flows may be written in tensor notations as:

$$\frac{\partial}{\partial x_i}(\rho \overline{u}_i \overline{u}_j) = -\frac{\partial \overline{p}}{\partial x_i} + \frac{\partial}{\partial x_i}[(\mu_t + \mu)(\frac{\partial \overline{u}_i}{\partial x_j} + \frac{\partial \overline{u}_j}{\partial x_i} - (2/3)\delta_{ij}\frac{\partial \overline{u}_m}{\partial x_m}) - 2/3\rho\delta_{ij}k] \tag{2}$$

where, $\overline{u}_i$ and ρ are time-mean velocity components and density. The laminar and turbulent viscosities are denoted by μ and μ_t.

2.2 Turbulence model

The turbulent viscosity can be computed with the help of the two-equation model of turbulence for the kinetic energy of turbulence (k) and its dissipation rate (ε). The governing equations for the kinetic energy of turbulence and its dissipation rate are written here such that they can be applied to the standard k-ε model (Launder and Spalding [10]) or its low Reynolds number version of Launder and Sharma [11].

$$\frac{\partial}{\partial x_i}\left(\rho u_i k\right)-\frac{\partial}{\partial x_i}\left(\frac{\mu_e}{\sigma_k}\frac{\partial k}{\partial x_i}\right)=G-\rho\left(\varepsilon+D\right) \tag{3}$$

$$\frac{\partial}{\partial x_i}\left(\rho u_i \varepsilon\right)-\frac{\partial}{\partial x_i}\left(\frac{\mu_e}{\sigma_\varepsilon}\frac{\partial \varepsilon}{\partial x_i}\right)=\left(C_1 f_1 G-C_2 f_2 \rho\varepsilon\right)\frac{\varepsilon}{k}+\rho E \tag{4}$$

where, $G=\mu_t\left(\overline{u}_{i,j}+\overline{u}_{j,i}\right)\overline{u}_{i,j}-2/3\overline{u}_{m,m}\left(\mu_t\overline{u}_{m,m}+\rho\overline{k}\right)$ is the turbulence kinetic energy generation term and is given by Launder and Spalding [10]. The turbulent viscosity μ_t is thus given as:

$$\mu_t=C_\mu f_\mu \rho k^2/\varepsilon \tag{5}$$

The high Reynolds number standard k-e model is specified with the effective viscosity $\mu_e=\mu_t$, $D=E=0.0$ and $f_1=f_2=f_\mu=1.0$. Moreover, the high Reynolds number k-ε model logarithmic wall functions that prescribe the wall shear stress, the generation term (G) and the value of ε are given by Launder and Spalding [10].

However, the low Reynolds number k-ε model of Launder and Sharma [11] takes the solution right to the pipe wall. The common constants between the two versions of the k-ε model are given by Launder and Sharma [11] as $c_\mu=0.09$, $c_1=1.44$, $c_2=1.92$, $\sigma_k=1.0$ and $\sigma_e=1.3$. Moreover, the low Reynolds number additional functions are defined as follows [11]:

$$f_\mu=\exp\left[-3.4/\left(1+R_t/50\right)^2\right] \tag{6}$$

$$f_1=1.0 \tag{7}$$

$$f_2=1-0.3\exp\left(-R_t^2\right) \tag{8}$$

$$D = 2\left(\mu / \rho\right)\left[\frac{\partial(k)^{\frac{1}{2}}}{\partial r}\right]^2 \tag{9}$$

$$E = 2\left(\mu / \rho\right)\left(\mu_t / \rho\right)\left[\frac{\partial^2 u}{\partial r^2}\right]^2 \tag{10}$$

where, the turbulent Reynolds number R_t is defined as [10, 11]

$$R_t = \rho k^2 / \left(\mu\varepsilon\right) \tag{11}$$

Equations (9) and (10) are given specifically for the turbulent flow in pipes where r is the radial distance and u is the axial velocity.

In the low Reynolds number model, μ_e is defined as $\mu + \mu_t$ and the wall boundary condition is defined as $\partial p'/\partial r = u = v = k = \varepsilon = 0.0$. The boundary condition at the centerline is defined as $\partial\phi/\partial r = v = 0$, where ϕ stands for all dependent variables except v. At the exit section, the axial gradients of all dependent variables are equal to zero. At the inlet section, $u = u_{\text{in}}$ and $v = \partial p'/\partial x = 0$, where u_{in} is the inlet uniform axial velocity and p' is the pressure correction.

2.3 Energy equation

The energy equation for the turbulent flow in pipes is written as:

$$\frac{\partial}{\partial x_i}(\rho\bar{u}_i\bar{T}) - \frac{\partial}{\partial x_i}\left[(\mu/\mathrm{Pr} + \mu_t/\mathrm{Pr}_t)\frac{\partial\bar{T}}{\partial x_i}\right] = 0 \tag{12}$$

Where, Pr and Pr_t are the laminar and turbulent Prandtl numbers. For air, which is the working medium in the present work, the laminar and turbulent Prandtl numbers are taken as 0.7 and 0.7.

The above governing equations are solved iteratively using the higher-order scheme of Abou-Ellail et al. [3]. For a 100x100 mesh, 5000 iterations are required for complete conversion of the difference equations of the velocity components, pressure correction, air temperature, k and ε.

3 Presentation and discussion of results

The results presented below are the outcome of six individual simulations for an inlet temperature of 300 K and Reynolds numbers (Re) of values 31260, 62510, 93770, 125000, 15630 and 187500. The pipe is 200 cm long and its diameter (D) is 5 cm. Figure 1 depicts the axial profiles of the Nusselt number (Nu) along the pipe axis for the above values of Reynolds numbers (Re). For a fixed value of Re, the Nusselt number decreases sharply near the inlet section to reach a minimum value then increases gradual toward the pipe exit section, where Nu reaches its fully-developed value. The dip in the Nu- x/D curves occurs around

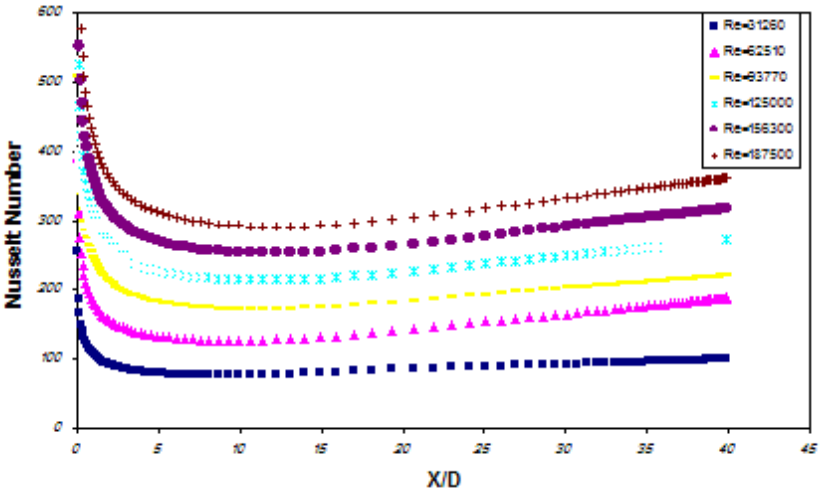

Figure 1: Axial Nusselt number profiles along the pipe axis, at different Reynolds numbers, for a constant wall temperature of 400 K.

an axial distance of approximately 14 to 18 pipe diameters, where u approaches its fully developed value.

Figure 2 shows the axial profiles of the local turbulent heat transfer coefficient along the pipe axis for different values of the Reynolds number. The curves of Fig. 2 are almost a replica of the curves of Fig. 1, since the thermal

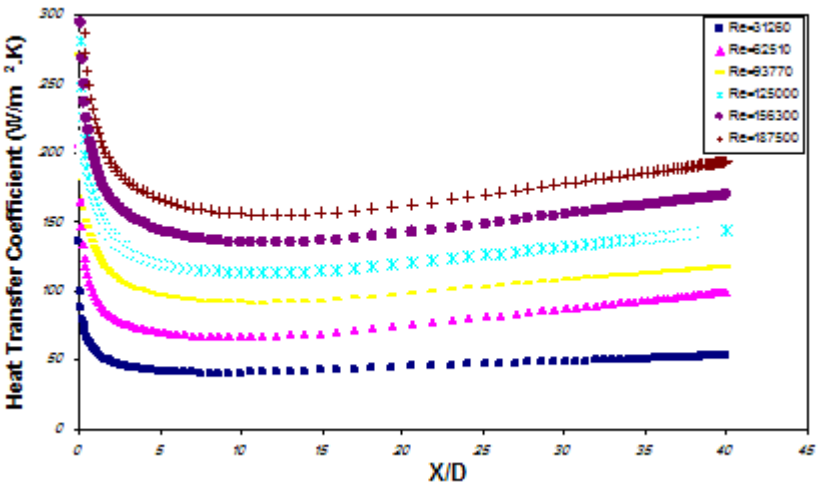

Figure 2: Axial profiles of the local turbulent heat transfer coefficient along the pipe axis, for different Reynolds numbers.

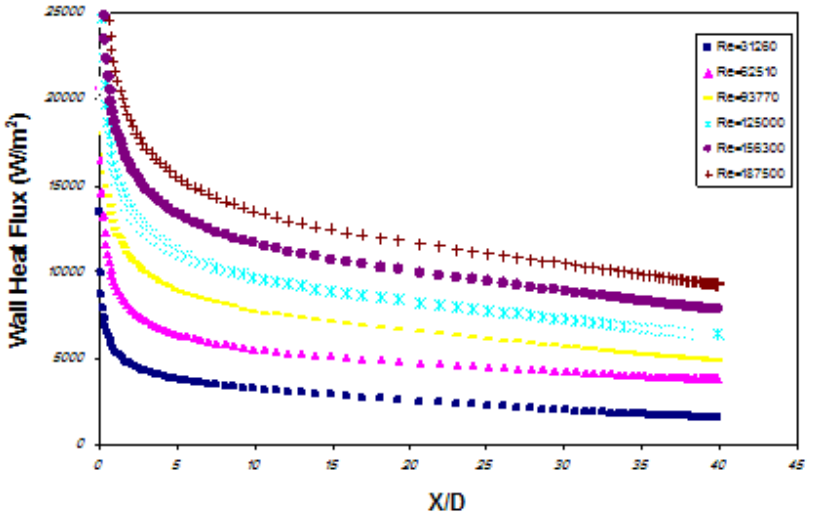

Figure 3: Axial profiles of the local wall heat flux along the pipe axis, for different values of Reynolds number.

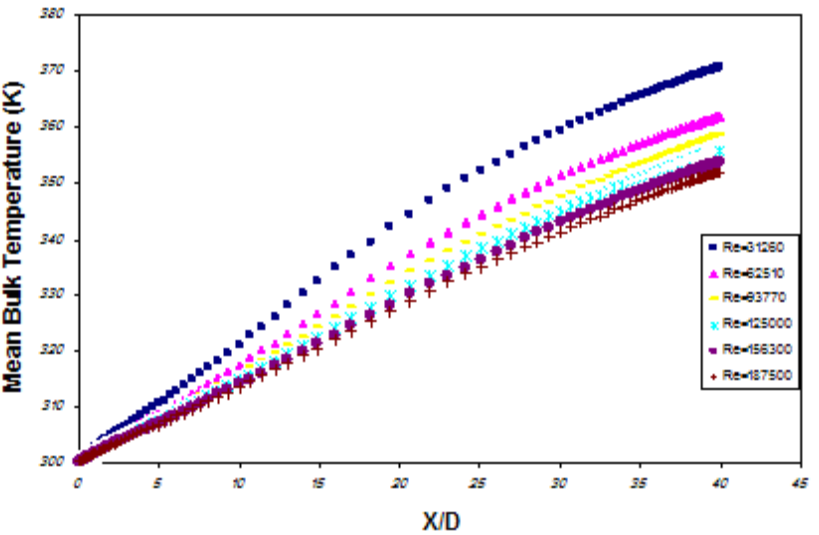

Figure 4: Axial profiles of the local mean bulk temperature along the pipe axis, for different values of Reynolds number.

conductivity is practically constant in the temperature range of 300 K to 400 K. Therefore, the comments on Fig. 1 apply to Fig. 2. The local wall heat flux is plotted in Fig. 3 against the dimensionless axial distance. It should be mentioned here that the wall heat flux is computed from the thermal conductivity and the radial temperature gradient at the wall, for a wall temperature of 400 K. No wall function is thus needed when using a low Reynolds number $k-\varepsilon$ model. The wall heat flux decreases sharply at the pipe entrance section followed by a much slower decay as the exit section is approached.

Figure 4 depicts the axial variations of the mean bulk temperature, for *Re* = 31260, 62510, 93770, 125000, 156300 and 189500. At low Reynolds numbers the mean bulk temperature increases linearly, while at high Reynolds number the linearity is not so clear. The dip in the Nusselt number of Fig. 1 becomes obvious from comparing the decrease of the heat flux and the increase of the mean bulk temperature. It is thus clear from Figs. 3 and 4 that eventually the Nusselt number will start to increase as the pipe exit section is approached.

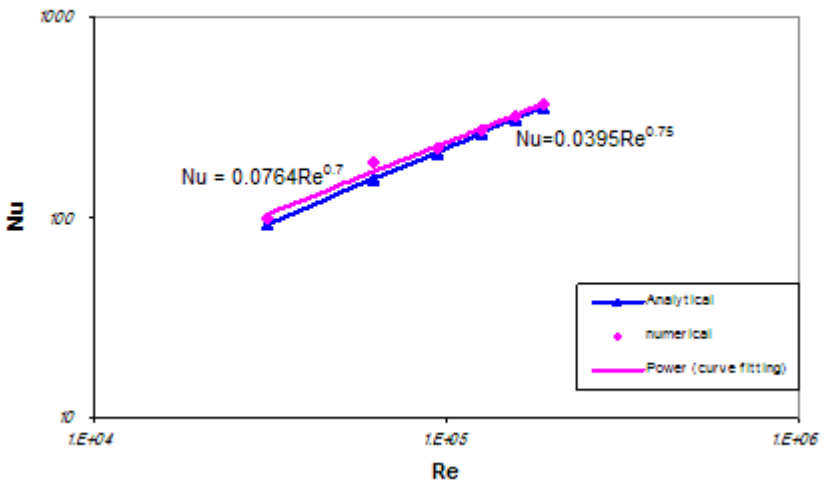

Figure 5: Variation of the fully-developed Nusselt number versus Reynolds number for turbulent flow in pipes. Holman equation [15] is included.

The fully-developed *Nu* versus *Re* is depicted in Fig. 5. The present numerical results are compared with the corresponding analytical equation of Holman [15]. The agreement between the low Reynolds number model results and Holman's equation is very good, suggesting that it is time to abandon the wall functions for the flow and heat transfer. The present results can be correlated as:

$$Nu = 0.0764\,\mathrm{Re}^{0.7} \tag{13}$$

It should be mentioned here that Holman's equation ($Nu = 0.0395\,\mathrm{Re}^{0.75}$) was obtained for turbulent flows in pipes with constant wall heat flux and unity Prandtl number

Figure 6 shows the radial profiles of the axial velocity for *Re*=31260. Similarly the radial profiles of the temperature are depicted in Fig. 7. For *x/D* = 13.9, the axial velocity is nearly fully developed, while the temperature continues to change up to the pipe exit section. It can be seen from Fig. 8 that the low Reynolds number model predicts accurately the fully-developed pipe flow, while the standard $k-\varepsilon$ deviate from the experimental data near the pipe wall.

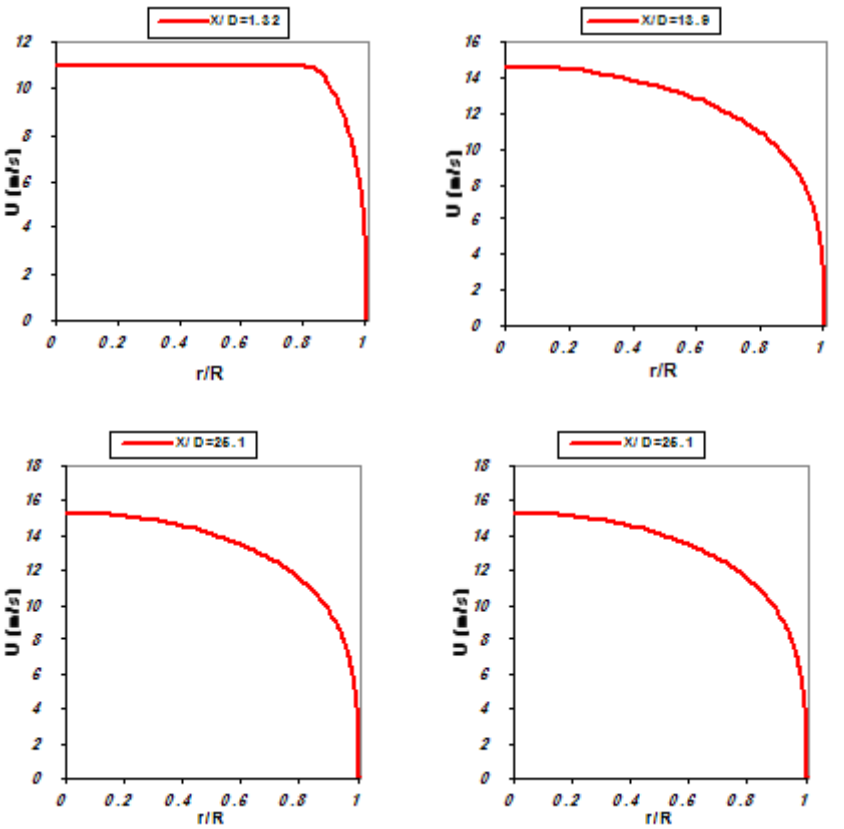

Figure 6: Axial velocity radial profiles at different axial distances, for a Reynolds number value of 31260.

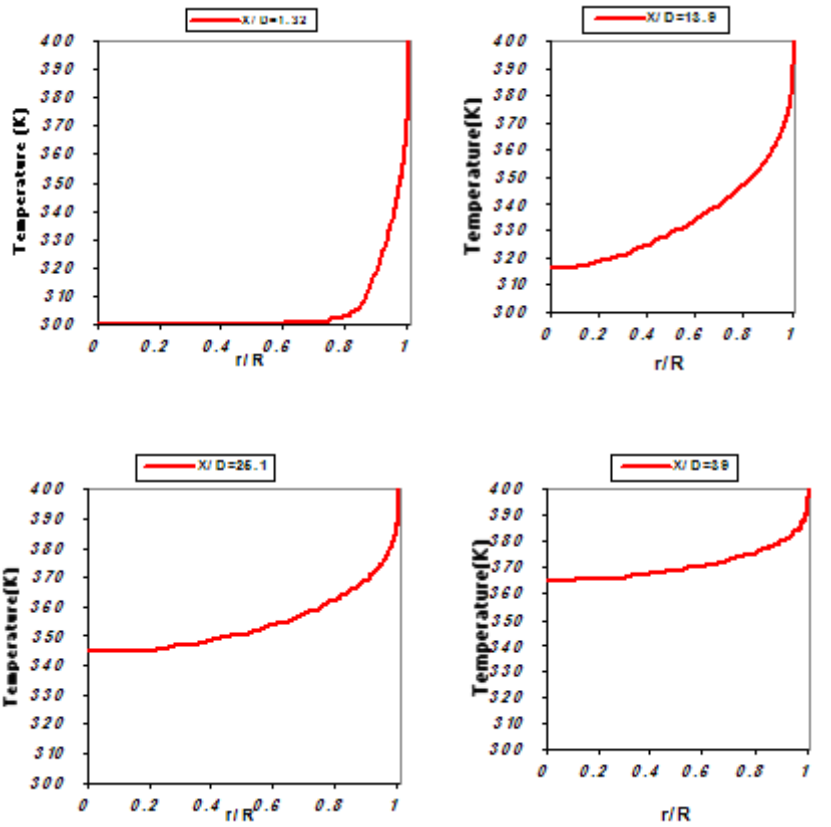

Figure 7: Radial temperature profiles at different axial distances, for a Reynolds number value of 31260.

4 Conclusions

The numerical results for the turbulent flow and heat transfer in pipes is presented. A low Reynolds number $k-\varepsilon$ model is utilized. No wall functions are used for the fluid flow or the heat tarnsfer. The present results show clearly that the computed axial velocity and Nusselt number are in good agreement with the experimental data and the sim-emperical corrolations. A dip in the axial profiles of the Nusselt number is noticed that could be atributed to the faster development of the axial velocity in comparison to the gas temperature.

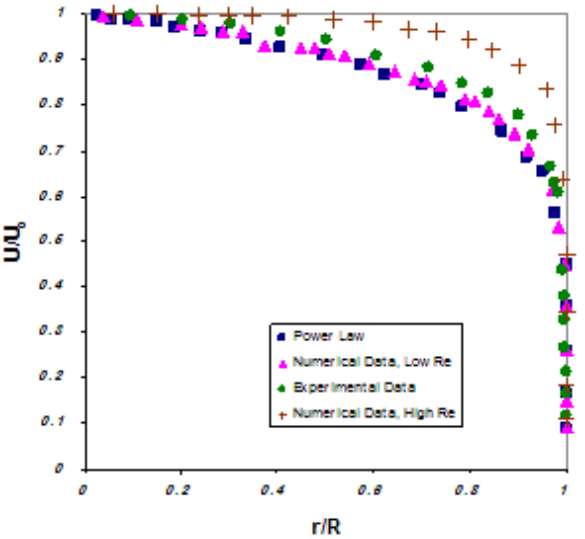

Figure 8: Dimensionless fully-developed axial velocity radial profiles, for Re = 500,000, using low Reynolds number model [10] and the high Reynolds number $k-\varepsilon$ model. Experimental data [13] and the $1/7^{th}$ power law [14] are also included.

References

[1] Abou-Ellail, M.M.M., Gosman, A.D., Lockwood, F.C., Megahed, I.E.A., Description and validation of a three-dimensional procedure for combustion chamber flows. *AIAA Journal of Energy,* **2**, pp. 71–80, 1978.

[2] Patankar, S.V., *Numerical Heat Transfer and Fluid Flow*. McGraw Hill: New York, 1980.

[3] Abou-Ellail, M., Li, Y. & Tong, T., A Novel Non-Upwind Interconnected Multi-Grid Overlapping Numerical Procedure for Problems Involving Fluid Flow. *International Journal for Numerical Methods in Fluids*. **57(11)**, pp. 1669-1694, 2008.

[4] Leonard, B.P., Stable and Accurate Convective Modeling Procedure Based on Quadratic Upstream Interpolation. *Computer Methods in Applied Mechanics and Engineering*, 19, pp. 59–98, 1979.

[5] Leonard, B.P., A Stable, Accurate, Economical and Comprehendible Algorithm for the Navier-Stokes and Scalar Transport Equations. *Numerical Methods in Laminar and Turbulent Flow*, eds. C. Taylor & B.A. Schrefler, *Proceedings of the Second International Conference*, pp. 543–553. Venice, Italy, 1981.

[6] Song, B., Liu, G.R., Lam, K.Y. & Amano, R.S., On a Higher-Order Bounded Discretization Scheme. *International Journal for Numerical Methods in Fluids*, **32**, pp. 881–897, 2000

[7] Song, B., Liu, G.R. & Amano R.S., Applications of a Higher-Order Bound Numerical Scheme to Turbulent Flows. *International Journal for Numerical Methods in Fluids*, **35**, pp. 371–394, 2001.
[8] Raithby, G.D., Skew Upstream Differencing Schemes for Problems Involving Fluid Flow. *Computer Methods in Applied Mechanics and Engineering*, **9**, pp. 153–164, 1976.
[9] Verma, A.K. & Eswaran, V., Overlapping Control Volume Approach for Convection-Diffusion Problems. *International Journal for Numerical Methods in Fluids*, **23**, pp. 865–882, 1996.
[10] Launder, B. & Spalding, D., The numerical computation of turbulent flows. *Computer Methods in Applied Mechanics and Engineering* **3**, pp. 269-289, 1974.
[11] Launder, B. & Sharma, B., Application of the energy-dissipation model of turbulence to the calculation of flow near a spinning disc, *Letters in Heat and Mass Transfer,* **1**, pp. 131-137, 1974.
[12] Hrenya, C. M., Bolio, E. J., Charkrobarti, D. & Sinclair, J.L., Comparison of Low Reynolds Number $k-\varepsilon$ Turbulence Models in Predicting Fully Developed Pipe Flow. *Chemical Engineering Science*, **50**, No. 12, pp. 1923-1941, 1995.
[13] Laufer, J., The structure of turbulence in fully developed pipe flow. *NACA*, report no. 1174, 1954.
[14] Schlichting, H*., Boundary-Layer Theory*, Chapter 20, McGraw-Hill Book Company, New York, 1979.
[15] Holman, J.P., *Heat Transfer*, Chapter 5, McGraw-Hill Book Company, New York, 1997